ISSN: 2447-3359

REVISTA DE GEOCIÊNCIAS DO NORDESTE

Northeast Geosciences Journal

v. 6, nº 2 (2020)

https://doi.org/10.21680/2447-3359.2020v6n2ID19406

PETROGRAPHY AND LITHOCHEMISTRY OF MIGMATITIC ROCKS IN THE NORTH PORTION OF THE SALVADOR-ESPLANADA-BOQUIM BELT, SÃO FRANCISCO CRATON, BRAZIL

Marcus Vinicius Costa Almeida Junior[1]; Angela Beatriz de Menezes Leal[2]; Johildo Salomão Figuerêdo Barbosa[3]; Moacyr Moura Marinho[4]

[1]Mestre em Geologia, Programa de Pós-Graduação em Geologia, Núcleo de Geologia Básica (NGB), Instituto de Geociências, Universidade Federal da Bahia (UFBA), Salvador-BA, Brasil.
ORCID: https://orcid.org/0000-0002-2742-5290
Email: mvcajr@gmail.com

[2]Doutora em Geologia, Programa de Pós-Graduação em Geologia, Núcleo de Geologia Básica (NGB), Instituto de Geociências, Universidade Federal da Bahia (UFBA), Salvador-BA, Brasil.
ORCID: https://orcid.org/0000-0003-1179-9877
Email: angelab@ufba.br

[3]Doutor em Geologia, Programa de Pós-Graduação em Geologia, Núcleo de Geologia Básica (NGB), Instituto de Geociências, Universidade Federal da Bahia (UFBA), Salvador-BA, Brasil.
ORCID: https://orcid.org/0000-0002-2277-1522
Email: johildo.barbosa@gmail.com

[4]Doutor em Geologia, Programa de Pós-Graduação em Geologia, Núcleo de Geologia Básica (NGB), Instituto de Geociências, Universidade Federal da Bahia (UFBA), Salvador-BA, Brasil.
ORCID: https://orcid.org/0000-0002-2143-5594
Email: mmm@ufba.br

Abstract

The study area is located in the extreme northern of the Salvador-Esplanada-Boquim Belt, in the southern portions of the state of Sergipe and northeastern state of Bahia, Brazil. This belt has three lithological groups of metamorphic rocks called Rio Real-Riachão do Dantas Migmatitic Complex (CMRR), Esplanada-Boquim Granulitic Complex (CGEB) and Gneissic/Granulitic-Migmatitic Atlantic Coast Complex (CGGCA). This article is limited to the petrological study of the first migmatites group that has been subdivided into East Granitic Migmatitic Orthogneisses (OMGL) and WestGranitic Migmatitic Orthogneiss (OMGO). Both, macroscopically and petrographically are similar, whose mineral parageneses indicate the occurrence of metamorphic processes of medium grade, from the amphibolite facies with retrometamórficas tracks. Lithochemically, it was noted particular characteristics of light and dark portions from these types of migmatites and that, although they have suffered migmatisation, kept also the characteristics of the protolith, allowing identify the felsic portions as from magma ranging from calc-alkaline regular to calcium-alkaline of the high K.

Keywords: Salvador-Esplanada-Boquim Belt, Lithochemistry, Petrography.

PETROGRAFIA E LITOQUÍMICA DAS ROCHAS MIGMATÍTICAS DA PORÇÃO NORTE DO CINTURÃO SALVADOR-ESPLANADA-BOQUIM, CRÁTON DO SÃO FRANCISCO, BRASIL

Resumo

A área de estudo localiza-se na porção extremo norte do Cinturão Salvador-Esplanada-Boquim, nas porções sul do estado de Sergipe e nordeste do estado da Bahia, Brasil. Este Cinturão apresenta três faixas litológicas de rochas metamórficas denominadas Complexo Migmatítico Rio Real-Riachão do Dantas (CMRR), Complexo Granulítico Esplanada-Boquim (CGEB) e Complexo Gnáissico/Migmatítico-Granulítico Costa Atlântica (CGGCA). Esse artigo se restringe aos estudos petrológicos da primeira faixa de migmatitos que foi subdividida em Ortognaisse Migmatítico Granítico Leste (OMGL) e Ortognaisse Migmatítico Granítico Oeste (OMGO). Ambas, macroscopicamente e petrograficamente são similares, cujas paragêneses minerais indicam a ocorrência de processos metamórficos de médio grau, da fácies anfibolito com faixas retrometamórficas. Litoquimicamente, notou-se características particulares das porções claras e escuras de cada um desses tipos de migmatitos e que, embora tenham sofrido migmatização, mantiveram as características dos protólitos, permitindo identificar as porções félsicas como provenientes de magma variando entre cálcio-alcalino normal a cálcio-alcalino de alto K.

Palavras-chave: Cinturão Salvador-Esplanada-Boquim, Litquímica, Petrografia

PETROGRAFÍA Y LITOQUÍMICA DE LAS ROCAS MIGMÁTICAS DE LA PORCIÓN NORTE DEL CINTURÓN SALVADOR-ESPLANADA-BOQUIM, CRATON DEL SÃO FRANCISCO, BRASIL

Resumen

El área de estudio se encuentra en el extremo norte del Cinturón Salvador-Esplanada-Boquim, en las partes meridionales del estado de Sergipe y el estado nororiental de Bahía, Brasil. Este cinturón tiene tres grupos litológicos de rocas metamórficas llamadas Complejo Migmatítico Rio Real-Riachão do Dantas (CMRR), Complejo Granulítico Esplanada-Boquim (CGEB) y Complejo Gneissico / Granulítico-Migmatítico de la Costa Atlántica (CGGCA). Este artículo se limita al estudio petrológico del primer grupo de migmatitas que se ha subdividido en Ortogneises Migmatíticos Graníticos Este (OMGL) y Ortogneis Migmatíticos Migratorios Oeste (OMGO). Ambos, macroscópicamente y petrográficamente son similares, cuyas paragénesis mineral indican la ocurrencia de procesos metamórficos de grado medio, a partir de las facies de anfibolitos con pistas retrometamórficas. Litoquímicamente, se observaron características particulares de las porciones claras y oscuras de estos tipos de migmatitas y que, aunque han sufrido migmatización, mantuvieron también las características del protolito, lo que permitió identificar las porciones felsicas como del magma que van desde el calcio alcalino regular al calcio - alcalino de la alta K.

Palabras-clave: Cinturón Salvador-Esplanada-Boquim, Litoquímica, Petrografía.

1. INTRODUCTION

The São Francisco Craton (CSF) consists of gneissic, granitic, granulitic and migmatitic terrains with ages varying from the Archean to the Paleoproterozoic, overlaid by a meso to Neoproterozoic paraplatform cover (BARBOSA et al., 2012). Its geological history is based on tectonic, magmatic and metamorphic events in addition to erosive and exhumation processes, being assimilated by a broad evolutionary context, corresponding to one of the best and most complete geological records of the Brazilian Precambrian (HASUI, 2013) (Figure 01).

At the northern limit of this craton, appears the rocks belonging to the Salvador-Esplanada-Boquim Belt (CSEB), consisting of orthogneisses of varied composition, rebalanced in granulite and amphibolite facies, in addition to calc-silicates, quartzite, granite, body intrusions and mafic/ultramafic rocks (BARBOSA, 1990; SANTOS et al., 2001; OLIVEIRA, 2014).

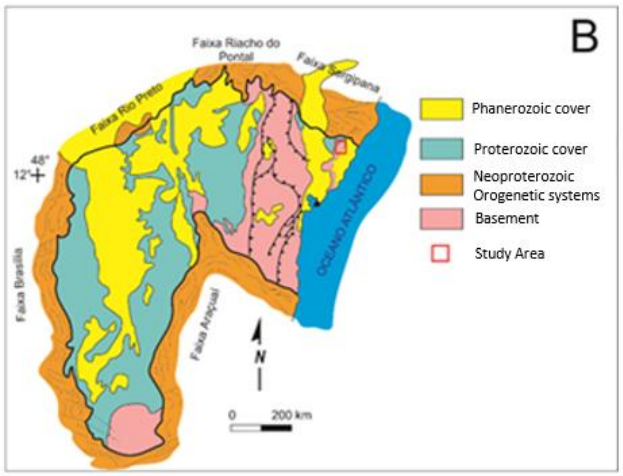

Figure 01 – São Francisco Craton, with delimitation of the study area. (Modified from Alkmim et al., 1993)

The CSEB refers to a set of Archean-paleoproterozoic rocks, metamorphised to a high degree, occurring from the eastern edge of the Recôncavo-Tucano-Jatobá sedimentary basin, represented lithologically by three relatively continuous bands of metamorphic rocks, delimited by faults in pushing and / or shear zones with transcurrent plans, which produced structuring of NNE direction (SANTOS et al., 2001; OLIVEIRA, 2014). These shears have regional and deep expression, registered by geophysics (OLIVEIRA JR., 1990; SANTOS et al., 2001; SILVA et al., 2002; BARBOSA et al., 2012; BARBOSA et al., 2018): (i) the first band, located to the west, called the Rio Real-Riachão do Dantas Migmatitic Complex (CMRR), extends from the south of Aporá to Riachão do Dantas, to the north, with migmatitic orthogneisses with folded, schlieren and stromatic structures and granitoids, besides the Granitoide Teotônio-Pela Porco Suite; (ii) the second, located in the central part, called Esplanada-Boquim Granulitic Complex (CGEB), extends from Esplanada to Boquim, containing granulites with basic enclaves, kinzigite levels and subordinate quartzite lenses, and (iii) the third, located to the east, called Gnaissico/Migmatítico-Granulítico Costa Atlântica Complex (CGGCA), which extends from the surroundings of the city of Conde extending towards the north to the Atlantic Coast, with highlighting lithologies of the bimodal orthogneisses type, sometimes migmatized, presenting tonalitic-granodioritic and mafic terms, not excluding the presence of sieno-monzogranitic intrusions and granulitic nuclei. Both, the first and second bands, are crossed by acidic to intermediate dykes, the latter constituting Arauá's dikes (SANTOS et al., 2001; D'EL-REY SILVA, 2005). These lithologies, especially those in the second and third bands, are superimposed by the Barreiras Group sediments. This study prioritized the migmatitic rocks of the first band (CMRR).

The study area is located in the extreme north of the CSEB and aimed to characterize the medium to high grade gneissic-migmatitic rocks of this belt, taking into account petrographic and lithochemical aspects and maintaining the division proposed by Barbosa et al. (2018).

2. METHODOLOGY

For petrographic analysis, the thin sections were made at the Petrography Laboratory of CPRM - Companhia de Pesquisa e Recursos Minerales, in Salvador, Bahia, in addition to the adding of thin sections from the GEOTERM-NE Project (2010).

For the lithochemical studies, 49 samples were selected, 13 from fieldwork carried out during the research and 36 from the GEOTERM-NE Project (2010); all analyzed in the GEOSOL - Geologia e Sondagens Ltda laboratory, using lithium metaborate fusion methods (ICP-OES and ICP-MS). By the ICP-OES method, the contents of SiO_2, TiO_2, Al_2O_3, Fe_2O_3t, MnO, MgO, CaO, Na_2O, K_2O, P_2O_5, Cr_2O_3 were determined, in addition to the elements Ba, Sr, Y, Zr, V being the first in weight percentage and the last in ppm. By the ICP-MS method the elements Ce, Cs, Dy, Er, Eu, Gd, Hf, Ho, La, Lu, Nb, Nd, Ni, Pr, Rb, Sm, Ta, Tb, Th, Tm, U were determined , and Yb, all in ppm. The values of K, P and Ti were also calculated, in ppm, from the levels of their oxides. LOI was calculated by the difference in weight after heating 0.2 g of sample to 1000ºC and the analytical error is less than 5% for oxides and less than 2% for trace elements.

3. RESULTS AND DISCUSSION

3.1. Macro and Microscopic Aspects

As can be seen in figure 02, in the Rio Real-Riachão do Dantas Migmatitic Complex (CMRR) of the CSEB, in the study area, there are basically two types of migmatites: in the eastern portion, in contact with the Esplanada-Boquim Granulitic Complex (CGEB), the Eastern Granitic Migmatitic Orthogneiss (OMGL) and the Western Granitic Migmatitic Orthogneiss (OMGO) are located to the west.

3.1.1. Eastern Granitic Migmatitic Orthogneiss (OMGL)

Corresponds to granitic-gneissic rocks, of medium to coarse granulometry, grayish color, with variations in tones due to the greater or lesser amount of the biotite mineral, in addition to compositional banding, characteristic of this unit (Figure 03A). The occurrence of leucosome pockets included in the paleosome is observed, and the whole set is affected by ductile deformation (Figure 03B). Leucossomatic veins also occur, mainly composed of quartz and feldspars, as well as small granite portions showing diffuse contact with the embedding, possibly being an action of anatectic process. It is also observed in this migmatitic band the presence of orthogneisses with granite composition and incipient portions of migmatization.

Petrographically (Figures 03C and 03D), it mainly presents unequigranular and granular granoblastic microstructures and, secondarily, polygonal granoblastic, poikiloblastic sieve and lepidoblastic microstructures. It also identifies the presence of mimerquitic texture, with intergrowth of quartz and plagioclase, in addition to pertites and mesopertites, in varying proportions. In the samples collected near the Aporá-Itamira shear zone that separates the CMRR from the CGEB (Figure 02), it was possible to observe a granolepidoblastic microstructure and quartz and feldspar porphyroclasts immersed in a matrix composed of biotite, quartz, plagioclase and microcline. It was also possible to notice quartz-feldspar veins representing the leucosome of this unit. In modal terms, they consist of quartz (30-45%), plagioclase (20-30%), biotite (8-20%), microcline (5-15%), muscovite (2-10%), chlorite (2- 7%), hornblende (2-4%), opaque (1-5%), in addition to epidote, magnetite, hematite and zircon as accessory minerals, being classified as syeno to monzogranites, with a greater tendency to the second, according to Streckeisen's QAP diagram (1976) (Figure 05).

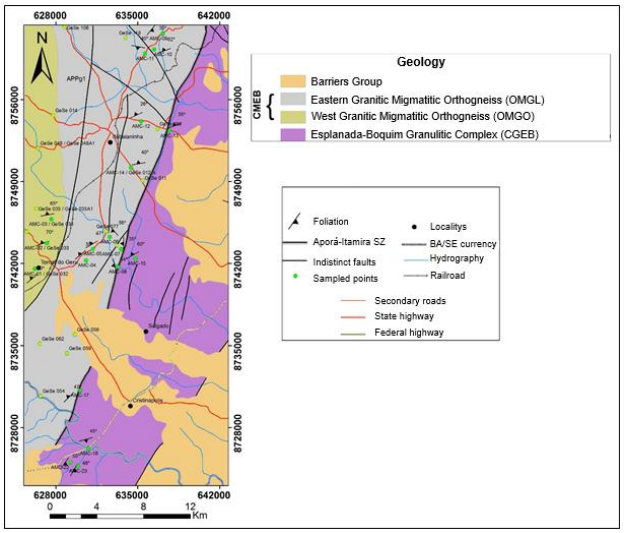

Figure 02 – Geological map of the study area. (Modified from GEOTERM-NE, 2010; BARBOSA et al., 2018)

3.1.2. West Granitic Migmatitic Orthogneiss (OMGO)

They are orthoderivated migmatites of granitic composition, presenting well-characterized migmatites in several stages of partial fusion, from metathexites with well-marked banding to nebulitic diatexites, in addition to the occurrence of leucossomatic pegmatoid pockets, composed basically of quartz and feldspars (Figures 04A and 04B). The mesosome was hierarchized as a grayish-colored gneissic rock, well-marked foliation and medium granulometry; the neosome was considered to be representative of the melanosomatic phase, rich in biotite. There are also occurrences of more homogeneous portions, suggesting that it is the plutonic protolith of the rock.

Petrographically (Figure 04C and 04D), they present unequigranular and granular granoblastic microstructures, in addition to polygonal granoblastic and sieve-type poikiloblastic. The lepidoblastic microstructure occurs to a lesser extent, as well as mimerquitic and pertitic. Its mineralogical constituents are composed of quartz (30-35%), orthoclase (20-25%), plagioclase (12-20%), microcline (7-15%), biotite (3-15%), muscovite (3-9%), chlorite (2-10%), magnetite (1%), hematite (1%) and opaque (2-5%), in addition to zircon as a trace. They were classified as predominantly syenogranitic, with few samples tending to monzogranitic, according to the Streckeisen (1976) QAP diagram (Figure 05).

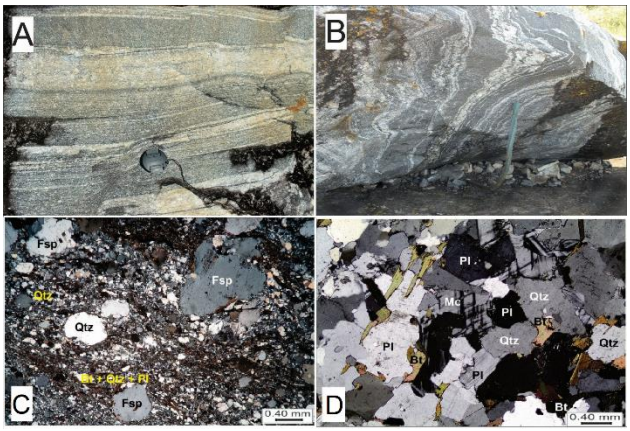

Figure 03 – OMGL field features and photomicrographs. (A) Compositional banding; (B) Presence of stromal leucosome in rock with a process of migmatization; (C) General aspect of the porphyroclastic microstructure with quartz and K-feldspar clasts immersed in an uneven granolepidoblastic matrix consisting of biotite, quartz and plagioclase. Total increase: 40x; (D) Granoblastic to slightly lepidoblastic rock consisting of plagioclase, quartz, microcline, and biotite. Total increase: 40x. Abbreviations according to Whitney and Evans (2010).

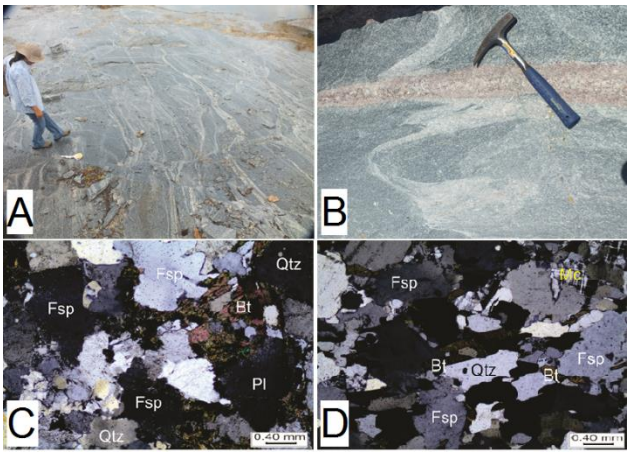

Figure 04 – OMGO field features and photomicrographs. (A) Nebulitic migmatitic features characteristic of this unit; (B) Evidence of leucossomatic pockets, younger than the embedding, rich in quartz and K-feldspar; (C) Granoblastic microstructure consisting of plagioclase, K-feldspar, quartz and biotite. Total increase: 40x; (D) Same as above. Abbreviations according to Whitney and Evans (2010).

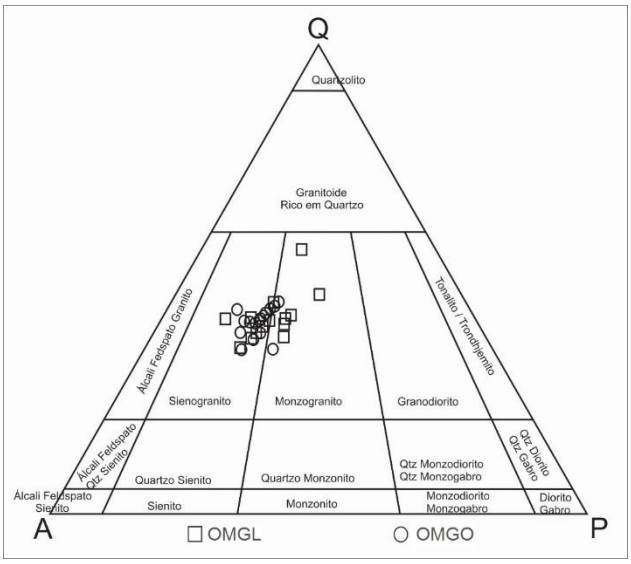

Figure 05 – QAP diagram (STRECKEISEN, 1976) for the samples of the two units analyzed.

3.2. Lithochemistry

The lithochemical characterization of this research takes into account the data referring to the major, trace and rare earths elements, which allowed the elaboration of classification diagrams, binary, ternary and multi-element diagrams, aiming at interpreting the lithochemical behavior of each unit and, alternatively, when possible, identify the magmatic series or series in addition to the probable environment in which the protholites of migmatites were formed. The table containing the lithochemical data can be seen in appendices 01 and 02.

3.2.1. Major Elements

Rocks in the OMGL domain have SiO_2 content ranging from 65.68% to 78.61%, Na_2O between 2.59% and 4.99%, Al_2O_3 from 11.11% to 18.42% and CaO ranging from 2, 9% to 1.18%, being classified as peraluminous, with A/CNK ranging from 1.38 to 2.21. In turn, rocks from the OMGO domain have SiO_2 levels ranging from 67.8% to 74.57%, Na_2O between 3.62% and 5.31%, Al_2O_3 from 13.56% to 16.36% and CaO varying. 1.26% to 2.81%. They exhibit an A/CNK ratio ranging from 1.40 to 1.60, which can be classified as peraluminous.

From the diagrams for the major elements (Figure 06), there are different patterns for the rocks of the OMGL and OMGO units, with negative correlations for TiO_2, P_2O_5, Al_2O_3, Na_2O and CaO. This behavior of Al_2O3 and CaO may be related to the crystallization of the protolith before migmatization. As a result, the possible simultaneous crystallization of K-feldspar and plagioclase phenocrystals must have been registered, indicating the possible fractionation of the latter. The behavior of TiO_2 may be related to titanite fractionation, as well as P_2O_5 with apatite. For K_2O, it's observes that in the OMGO unit, there is a positive correlation, evidencing the potassium character of these rocks, corroborating the syenogranitic character explained in figure 05. It is also observed that there is a greater dispersion of the

representative points of the samples from these migmatites that it is considered the result of migmatization. Indeed, it appears that the samples from the OMGO unit underwent more important migmatization than the OMGL unit since in the latter the points still remain with a certain organization reflecting more the characteristics of the protolith.

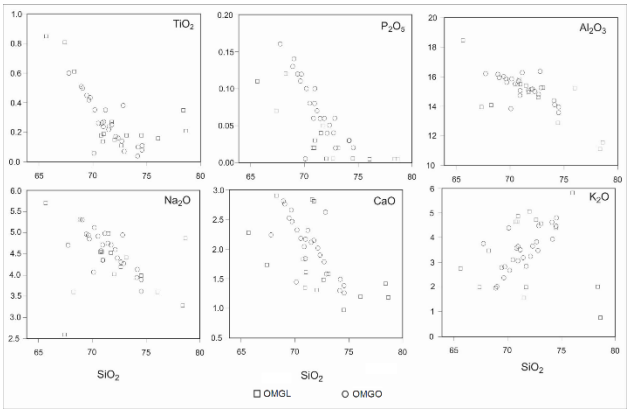

Figure 06 – Diagrams of chemical variation for the major elements for the two units studied.

Analyzing the diagram by Peccerillo and Taylor (1976) (Figure 07), it is possible to observe, for OMGL rocks, the existence of two series: the first calc-alkaline and the second high K calc-alkaline, which may suggest a evolutionary series between low and high K, that is, more enriched and less enriched samples in this element. Furthermore, despite the dispersion of the samples, one can infer the incipient occurrence of fractional crystallization of the protholites of these migmatites. OMGO rocks, similarly to the previous ones, present two well-defined patterns: the first occupying the field of the calc-alkaline series and the second, the field of the high-K calc-alkaline series, with a linear evolution of K_2O enrichment.

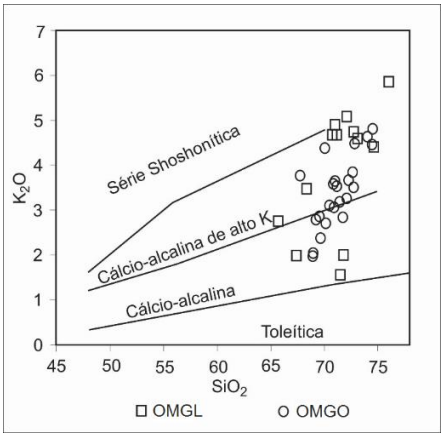

Figure 07 – SiO_2 versus K_2O diagram proposed by Peccerillo and Taylor (1976) for the two units studied.

According to O'Connor's (1965) ternary diagram (Figure 08A), OMGL rocks occupy granite fields with a tendency for granodiorites, while OMGO rocks lodge in the granite field, although they show evidence that the rocks less evolved can be linked with trondhjemites.

From the Na-K-Ca diagram by Barker and Arth (1976) (Figure 08B), with the insertion of the compositional field of Martin's Archean TTG's (1994), it is observed that the rocks of the two units, OMGL and OMGO, accompany the normal calc-alkaline trend, showing a clear affinity with the homonymous series. Once again, it appears that the trends of the protholites of the two units start close to the trondhjemitic trend.

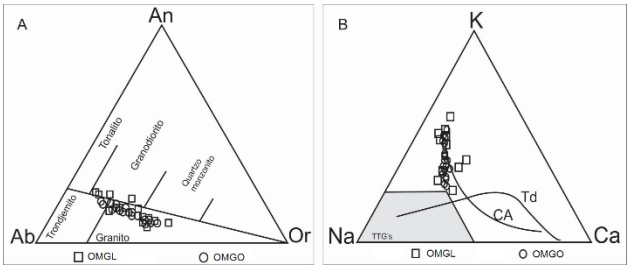

Figure 08 – A - Ab-An-Or ternary diagram, proposed by O'Connor (1965). B - Diagram Na-K-Ca (BARKER and ARTH, 1976), with a gray field referring to Martin's Archean TTG's (1994), CA: Calcium-alkaline trend. Td: trondjhemitic trend.

3.2.2. Trace and Rare Earth Elements

Trace elements from the rocks of the OMGL unit show enrichment in LILE (Large Ion Litophile Elements) and depletion in HFSE (High Field Strength Elements), in addition to negative anomalies in Ta, Nb and P and positive anomalies of U and Nd. Negative correlations suggest differentiation during protolith crystallization. In fact, despite the high rate of partial melting of these rocks, characteristics of the protolith remained after melting (Figure 09A). OMGO rocks unit have high K calc-alkaline characteristics, with LILE enrichment and HFSE depletion, in addition to the strong negative anomalies of Nb, Ta, Sr, P and Ti, the first two elements suggesting a reflection from the crustal source of the parental magma (Figure 09B). The variation in Sr levels may suggest the plagioclase fractionation. On the other hand, the positive anomalies of Th and Rb may suggest a continental crust involvement during the genesis of these rocks.

Observing the Rare Earth elements, the rocks of the OMGL unit present enrichment in ETRL (Light Rare Earth Elements) and depletion in ETRP (Heavy Rare Earth Elements), in addition to negative Eu anomaly, showing the accumulation of plagioclase (Figure 09C). Regarding the OMGO unit, there is a strong fractionation, without significant Eu anomalies, sometimes negative, indicating fractionation of feldspar during the fusion process, and sometimes positive, reflecting the accumulation of feldspar during crystallization (Figure 09D). The disharmonious behavior of ETRL suggests the importance of metasomatism in the formation of these migmatites.

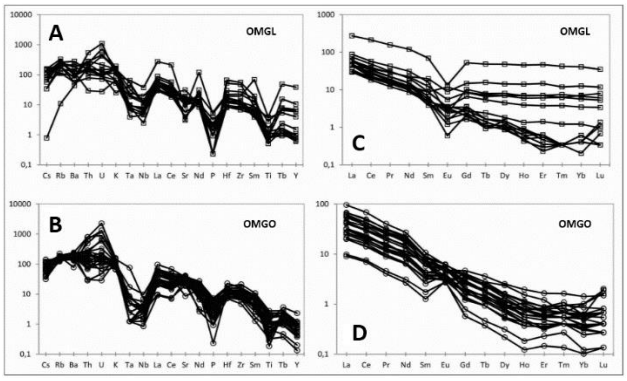

Figure 09 – A and B - Standardized multielementar diagrams for the primitive mantle of Sun and McDonough (1989) of the OMGL (A) and OMGO (B) units. C and D - Diagrams of the Rare Earth elements normalized to the primitive mantle of Sun and McDonough (1989) of the units OMGL (C) and OMGO (D).

3.2.3. Tectonic Ambience

From the binary diagram of Pearce et al. (1984) (Figure 10), it is observed that, for the rocks of the OMGL unit, the representative points of the chemical analyzes of the majority occupy the transition between the syn-collisional and volcanic arc environments, being more situated in this last field. The displacement of some samples to the syn-collisional field may be due to the chemical modifications of these rocks during migmatization, due to the enrichment of the chemical element Rb and the substantial presence of minerals such as feldspar and biotite. With regard to the rocks of the OMGO unit, they basically occupy the field of volcanic arch environment rocks.

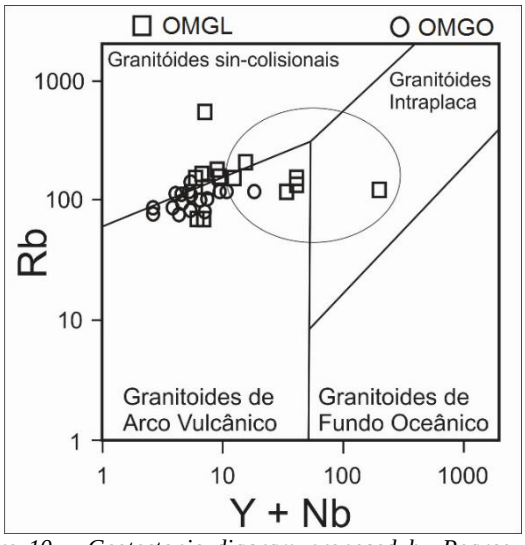

Figure 10 – Geotectonic diagram proposed by Pearce et al. (1984).

4. FINAL CONSIDERATIONS

The results obtained from this research have contributed to the geological knowledge of the northern portion of the Salvador-Esplanada-Boquim Belt (CSEB), bringing to light new information and relevant data on the origin and geological evolution of the region, some of which are interpreted in this article and others concluded and inserted in Barbosa et al. (2018).

In the field, it was found that the rocks of the study area show a higher degree of migmatization in its western portion, in the OMGO unit, decreasing the degree of these processes as you walk east, the OMGL unit.

Petrographically, similarities were observed in the composition of the two units, with small variations in the amounts of biotite, the type of existing plagioclase and the occurrence of accessory minerals. The relationship involving the rare clinopyroxenes, hornblende and brown/red biotite, should be indicative of lower metamorphism conditions in the region, corroborated by the punctual presence of the brownish-green hornblende and brown biotite. These minerals are common in areas of intense deformation process, in addition to the occurrence, in these areas, of other phyllosilicates (muscovite, chlorite). The maintenance of the division is reiterated, following the work of Barbosa et al. (2018).

Lithochemically, the OMGO unit presented rocks ranging from calc-alkaline to high-K calcium-alkaline, classified as being granitic, originating from an island arch environment, still with little post-collisional influence. According to the analysis of the major, trace and rare earths elements, it was concluded that the rocks of this unit underwent early crystallization of potassium feldspar and plagioclase phenocrystals, which were preserved during the partial melting of these rocks. These minerals also suggest the involvement of the continental crust during the formation of the protholites.

The rocks of the OMGL unit range from calc-alkaline to high-K calc-alkaline, associated with a volcanic to syn-collisional environment. The analysis of its major, trace and rare earths elements suggests the possibility of mixing magmas from different sources, as well as crustal contamination.

These rocks, therefore, would come from an island arch environment and, during their formation, differentiation and crustal contamination processes occurred. Thereafter, they were subjected to an intense process of migmatization during the metamorphic and retrometamorphic processes, which shaped their physical-chemical characteristics, as well as the lithochemical signatures.

5. REFERENCES

Alkmim F.F.; Brito Neves B.D.; Alves J.C.. Arcabouço tectônico do Cráton do São Francisco-uma revisão. In Dominguez, J.M.L.; Misi, A. (ed.) *O Cráton do São Francisco*. SBG-Núcleo BA/SE, 1993. 1, 45-62.

Barbosa, J.S.F.. The granulites of the Jequié complex and Atlantic mobile belt, southern Bahia, Brazil – An expression of ArcheanProterozoic plate convergence. In: Vielzeuf D. & Vidal P. (ed.). *Granulites and crustal evolution.* Clordrecht, Kluwer Académie, 1990. p. 195-221.

Barbosa, J.S.F.; Pinto, M.S.; Cruz, S.P.; Souza, J.S.. Terrenos Metamórficos do Embasamento, In Barbosa, J. S. F. (ed.) *Geologia da Bahia: pesquisa e atualização.* Série Publicações Especiais, 13 Convênio CBPM/UFBA-IGEO/SBG, 2012. 2v.

Barbosa, J.S.F.; Marinho, M.M.; Menezes Leal, A.B.; Oliveira, E.M.; Souza-Oliveira, J.S.; Argollo, R.M.; Lana, C.; Barbosa, R.G.; Santos, L.T.L.. As raízes granulíticas do cinturão Salvador-Esplanada-Boquim, Cráton do São Francisco, Bahia-Sergipe, Brasil. *Geologia USP. Série Científica*, 2018, 18(2), 103-128.

Barker, F.; Arth, J.G.. Generation of trondhjemitic-tonalitic liquids and Archaean bimodal trondhjemite-basalt suites. *Geology*, 1976. 4: 596-600.

D'el-Rey Silva, L.J.H.. New Sm-Nd data of (meta)sediments accross the São Francisco Craton-Sergipano Belt boundary, and from the Arauá dykes: Implications on Provenance Studies. In *III Simpósio sobre o Cráton do São Francisco*, Salvador, 14 a 18 de agosto de 2005, Anais III SCSF, 2005. p. 155-158.

GEOTERM-NE.. *Geração de calor nas bacias de Cumuruxatiba, Jequitinhonha, Sergipe-Alagoas e Pernambuco-Paraíba, e nos embasamentos a elas adjacentes.* Patrocinado pelo Promob-Cenpes-Petrobras e executado pelo CPGG-UFBA, 2010.

Hasui, Y.. Cráton São Francisco, *In* Almeida, F.F.M.; Bartorelli, A.; Carneiro, F.D.R.; Hasui, Y.; (eds.) *Geologia do Brasil.* Ed. Beca, São Paulo, 2013. 900p.

Martin, H.. The Archean grey gneisses and the genesis of the continental crust. In Condie, K.C. (ed.), *The Archean Crustal Evolution, Developments in Precambrian Geology*. Elsevier, Amsterdam, 1994. p. 205-259.

O'Connor, J.T.. A classification for quartz rich igneous rock based on feldspar rations. *USGS. Prof. Pap.*, 1965. 525B: 79–84.

Oliveira, E.M.. *Petrografia, litogeoquímica e geocronologia das rochas granulíticas da parte norte do Cinturão Salvador-Esplanada-Boquim, Bahia-Sergipe.* Tese de Doutorado, Programa de Pós Graduação em Geologia, Instituto de Geociências, Universidade Federal da Bahia, 2014. 220p.

Oliveira Jr., T.R.. *Geologia do extremo nordeste do Cráton São Francisco, Bahia.* Dissertação de Mestrado, Programa de Pós Graduação em Geologia, Instituto de Geociências, Universidade Federal da Bahia, 1990. 126p.

Pearce, J.A.; Harris, N.B.W.; Tindle, A.G.. Trace element discrimination diagrams for the tectonic interpretation of granitic rocks. *Journal of Petrology*, 1984. 25: 956-983.

Peccerillo, A.; Taylor, S.R.. Geochemistry of eocene calc-alkaline volcanic rocks from the Kastamonu area, northern Turkey. *Contributions to Mineralogy and Petrology*, 1976. 58: 63-81.

Santos, R.A.; Martins, A.A.M.; Neves, J.P.; Leal, R.A.. Programa Levantamentos Geológicos Básicos Do Brasil – PLGB. *Geologia e Recursos Minerais Do Estado De Sergipe. Escala 1:250.000. Texto Explicativo Do Mapa Geológico Do Estado De Sergipe.* Brasília: CPRM/DIEDIG/DEPAT; CODISE, 2001. 156p.

Silva, L.C.; Armstrong, R.; Delgado, I.M.; Pimentel, M.M.; Arcanjo, J.B.; Melo, R.C.; Teixeira, L.R.; Jost, H.; Pereira, L.H.M.; Cardoso Filho, J.M.. Reavaliação da evolução geológica em terrenos pré-cambrianos brasileiros, com base em novos dados U-Pb SHRIMP, Parte I: Limite centro-oriental do Cráton São Francisco na Bahia. *Revista Brasileira de Geociências*, 2002. 32(4): 501-512.

Streckeisen, A.. To each plutonic rock it's proper name. *Earth Science Review*, 1976. 12: 1-33.

Sun, S.S.; McDonough, W.F.. Chemical and isotopic systematic of oceanic basalts for mantle composition and process. In SAUNDER, A.D.; NORRY, M.J.; (ed.) *Magmatism in the ocean basins.* Geological Society, Special Publication, 1989. 42: 313–345.

Whitney, D.L.; Evans, B.W.. Abbreviations for names of rock-forming minerals. *American Mineralogist*, 2010. 95:185-187.

Received in: 04/12/2019
Accepted for publication in: 18/08/2020

Amostra	MV-10	MV-11	MV-12	MV-13	MV-16B	MV-17	GeSe 011	GeSe 012-A	GeSe 056	GeSe 059	GeSe 062	GeSe 077	GeSe 078-B	GeSe 092	GeSe 118
SiO_2	73,14	67,43	65,68	78,61	76,05	78,39	72,67	71,01	71,76	74,51	71,55	72,04	68,3	70,77	70,93
TiO_2	0,18	0,81	0,85	0,21	0,16	0,35	0,11	0,19	0,27	0,18	0,24	0,15	0,61	0,18	0,14
Al_2O_3	15,25	13,93	18,42	11,55	15,23	11,11	14,6	15,5	14,96	12,87	15,39	15,17	14,08	15,47	15,82
Fe_2O3_T	2,76	13,95	7,25	4,43	1,01	5,65	1,79	1,78	2,61	2,79	2,52	1,68	5,66	1,93	1,84
MnO	0,005	0,06	0,01	0,005	0,005	0,005	0,03	0,02	0,04	0,05	0,03	0,03	0,11	0,03	0,03
MgO	0,28	2,99	2,71	0,09	0,2	1,14	0,26	0,25	0,64	0,06	0,56	0,2	0,63	0,66	0,17
CaO	1,57	1,73	2,27	1,18	1,2	1,42	1,48	1,61	2,81	0,97	2,84	1,31	2,9	1,83	1,35
Na_2O	4,41	2,59	5,7	4,87	3,61	3,28	4,2	4,35	4,53	4	4,99	4,01	3,61	4,55	4,55
K_2O	4,55	1,99	2,75	0,75	5,81	2	4,71	4,86	1,99	4,39	1,55	5,05	3,47	4,65	4,65
P_2O_5	0,02	0,07	0,11	0,005	0,005	0,005	0,005	0,03	0,05	0,005	0,04	0,005	0,12	0,02	0,02
Cr_2O_3	0,005	0,03	0,02	0,01	0,005	0,005	0,001	-	0,001	0,001	0,001	-	-	-	0,001
LOI	0,39	0,97	0,6	0,41	0,35	0,78	0,14	0,38	0,33	0,19	0,27	0,37	0,29	0,49	0,49
Total	101,26	103,12	103,32	101,28	103,41	102,63	102,13	102,41	99,05	100,54	100,54	100,13	99,89	99,96	98,37
A/CNK	1,45	2,21	1,72	1,70	1,43	1,66	1,41	1,43	1,60	1,38	1,64	1,46	1,41	1,40	1,50
Cs	2,65	1,09	4,46	0,025	2,15	3,84	3,69	3,36	2,21	1,09	4,51	1,82	4,82	3,33	5,04
Rb	154,4	104,2	122,1	6,9	165,9	119,3	180,9	127	69,8	145,8	73,5	161	141	157,1	211
Ba	1245	857	540	304	1959	386	646	1529	641	1280	384	1314	936	1302	683
Th	23,8	2,5	46,1	15,3	11,9	13,4	15,4	13,6	13,1	19,3	6,7	20,5	10,6	8,9	23
U	4,51	0,58	23,22	1,92	1,81	2,88	8,83	3,06	1,83	2,45	1,52	15,31	2,2	1,9	9,75
Nb	7,37	4,57	26,82	8,83	1,75	8,14	5,85	3,93	3,56	9,6	3,27	5,27	13,95	3,29	8,6
Ta	2,21	0,41	2,67	1,85	0,36	0,76	0,38	0,32	0,34	0,85	0,26	0,38	1	0,16	1,37
La	50,9	20,4	187,6	30,5	32,6	21	20,2	38,7	23,5	60,3	30,6	41,9	41,6	31,4	31
Ce	85,3	40,2	376,2	64,4	51,2	36,1	32,1	57,4	36	100,8	38	60,8	69,5	41,8	47,5
Pr	8,47	4,5	43,14	7,83	5,19	4,05	3,34	6,06	3,9	11,63	4,25	6,18	7,95	3,95	4,77
Sr	262	118	165	71	339	85	279,8	380	292,4	64,5	413,2	257,5	226,1	658,3	216
Nd	27,4	15,8	162	30,2	16,9	16,9	11,5	20	13,8	41,9	14,1	20,5	29,8	13,2	16,7
Sm	3,9	3,8	30,7	8,7	2,1	3,9	2,1	2,4	2,1	7	1,7	2,9	5,4	2	2,5
Zr	140	88,1	218	619	116	531	75,6	154,9	142,2	304	117,2	121	256,3	95,1	141,6
Hf	5,36	2,5	6,01	20,59	3,62	16,19	2,63	4,91	4,18	9,14	4,27	4	6,86	2,93	5,5
Eu	0,57	0,58	2,25	1,49	0,2	1,98	0,28	0,48	0,6	0,39	0,57	0,26	0,92	0,1	0,4
Gd	2,05	3,95	31,11	8,81	0,97	4,99	1,4	1,25	1,67	6,1	1,16	2,14	5,09	1,28	1,63
Tb	0,1	0,58	5,21	1,68	0,12	0,71	0,15	0,1	0,18	0,85	0,12	0,18	0,79	0,12	0,26
Dy	1,08	3,31	35,22	10,5	0,64	5,16	0,7	0,77	0,94	5,92	0,63	1,09	5,13	0,83	1,34
Y	5	18	175	48	5	27	3,27	3,74	3,35	31,56	2,92	4,38	27,63	2,77	6,91
Ho	0,07	0,64	7,44	2,3	0,15	1,16	0,08	0,1	0,12	1,13	0,08	0,14	0,98	0,1	0,22
Er	0,14	1,8	22,41	7,03	0,26	3,37	0,11	0,3	0,3	3,38	0,26	0,22	2,91	0,17	0,68
Tm	0,025	0,28	3,12	0,88	0,025	0,46	0,025	0,025	0,025	0,55	0,025	0,025	0,46	0,025	0,09
Yb	0,1	1,7	20,1	6,2	0,2	3,5	0,2	0,3	0,2	3,3	0,2	0,2	2,8	0,2	0,6
Lu	0,05	0,25	2,58	0,87	0,08	0,59	0,025	0,025	0,025	0,45	0,08	0,1	0,39	0,025	0,07

Apêndice 01: Análises químicas em rocha total de elementos maiores (% em peso), traço (ppm) e terras raras (ppm) da unidade OMGL.

Amostra	MV-02	MV-04	MV-08	GeSe 014	GeSe 032A	GeSe 032A1	GeSe 032B	GeSe 032B1	GeSe 033A	GeSe 033A1	GeSe 033C	GeSe 034A
SiO_2	71,18	72,82	70,15	70,98	70,23	70,85	72,35	67,8	68,96	69,06	74,57	74,56
TiO_2	0,35	0,38	0,06	0,27	0,35	0,26	0,16	0,6	0,51	0,5	0,08	0,11
Al_2O_3	16,26	16,36	13,83	15,06	15,84	15,7	15	16,2	16,14	15,94	13,96	13,56
Fe_2O3_T	3,77	3,80	1,64	2,25	2,17	1,79	1,4	2,99	2,68	2,9	0,99	1,39
MnO	0,005	0,005	0,005	0,04	0,02	0,02	0,02	0,03	0,02	0,03	0,01	0,02
MgO	0,68	0,59	0,16	0,76	0,54	0,48	0,31	0,84	0,81	0,81	0,11	0,16
CaO	2,31	2,62	1,44	2,16	2,32	2,04	1,89	2,24	2,81	2,76	1,38	1,26
Na_2O	4,98	4,95	4,07	4,71	5,12	4,59	4,41	4,71	5,31	5,31	3,89	3,62
K_2O	3,51	3,48	4,38	3,05	2,68	3,57	3,64	3,75	1,95	2,02	4,45	4,79
P_2O_5	0,07	0,06	0,005	0,1	0,1	0,06	0,05	0,16	0,13	0,14	0,02	0,02
Cr_2O_3	0,005	0,01	0,005	0,001	0,001	0,001	0,001	0,001	0,001	0,001	0,001	0,001
LOI	0,25	0,24	0,18	0,4	0,4	0,4	0,05	0,4	0,4	0,3	0,3	0,3
Total	101,74	102,95	95,33	99,76	99,77	99,76	99,74	99,7	99,73	99,77	99,75	99,81
A/CNK	1,51	1,48	1,40	1,52	1,57	1,54	1,51	1,51	1,60	1,58	1,44	1,40
Cs	3,89	3,45	1,33	3,7	3,6	3,1	1,9	3,7	4,5	3,9	1,5	2
Rb	105,8	102,3	119	116,8	82,3	95,9	87,4	117,4	92,8	95,2	113,5	141,1
Ba	1406	1048	902	1262	1016	1416	1575	1397	964	941	1669	1088
Th	21,9	21,2	41,4	16,4	9,9	8,9	6,1	21,6	16,8	16,9	68	66,4
U	7,02	13,61	27,66	3,7	4,3	3,2	3,3	2,5	2,9	3,3	18,6	47,7
Nb	2,18	2,17	4,98	7	2,6	2,2	1,8	3,9	2,8	2,6	1	1,7
Ta	0,36	0,33	3,1	0,7	0,3	0,2	0,2	0,3	0,2	0,2	0,1	0,2
La	42,3	21,2	21,2	40,8	29,5	22,2	13,6	65,5	45,9	45,9	18,4	28,9
Ce	74,9	35,8	39,2	64,6	54,5	42,4	24,9	120,3	85,9	89	35	54,7
Pr	7,68	4,5	3,95	7,72	5,72	4,11	2,44	11,12	8,84	8,58	3,4	5,77
Sr	674	639	391	664	668,4	698,7	623	785,4	870	821,8	525,5	404,7
Nd	25,5	23,1	15,2	27,4	20,4	13,8	8,6	36,5	30,9	28,8	11,5	19,6
Sm	3,9	3,2	3,1	3,9	2,79	1,92	1,14	4,72	3,95	3,65	1,65	2,8
Zr	137	123	84	118,7	149,8	94,4	79,9	235,8	182,6	171,2	181,6	107
Hf	3,91	4,74	4,17	3,3	4,2	2,5	2,7	5,5	4,9	4,9	7	3,9
Eu	0,84	0,59	0,46	0,8	0,78	0,67	0,63	1,02	1,05	1,05	0,49	0,45
Gd	2,18	1,56	2,43	2,77	1,63	1,05	0,72	2,32	2,05	2,05	1,07	1,53
Tb	0,27	0,21	0,3	0,39	0,2	0,12	0,1	0,3	0,25	0,25	0,16	0,19
Dy	1,15	0,68	1,74	1,86	0,87	0,5	0,4	1,19	0,98	0,98	0,68	0,85
Y	5	5	5	10,5	4,2	2,3	2	5,5	4	4	3,5	3,5
Ho	0,18	0,17	0,25	0,32	0,13	0,07	0,07	0,19	0,13	0,13	0,13	0,13
Er	0,42	0,35	0,58	0,79	0,29	0,19	0,15	0,42	0,27	0,27	0,4	0,29
Tm	0,08	0,07	0,05	0,12	0,04	0,03	0,03	0,07	0,04	0,04	0,06	0,05
Yb	0,3	0,5	0,5	0,7	0,28	0,15	0,16	0,42	0,25	0,25	0,31	0,27

Lu	0,15	0,12	0,14	0,11	0,04	0,02	0,02	0,06	0,03	0,03	0,06	0,05

Apêndice 01: Análises químicas em rocha total de elementos maiores (% em peso), traço (ppm) e terras raras (ppm) da unidade OMGO.

Amostra	GeSe 034A1	GeSe 034B	GeSe 034C	GeSe 034E	GeSe 035	GeSe 035A1	GeSe 036A	GeSe 036A1	GeSe 036B	GeSe 048	GeSe 048A1
SiO_2	69,46	69,77	72,93	74,16	71,77	71,46	72,15	72,69	69,7	70,99	70,54
TiO_2	0,45	0,43	0,07	0,04	0,25	0,22	0,17	0,14	0,42	0,24	0,26
Al_2O_3	15,98	15,61	15,25	14,38	15,08	15,42	15,14	14,78	15,85	14,72	15,52
Fe_2O3_T	2,53	2,75	0,74	1,04	2,07	1,81	1,56	1,39	2,58	1,97	2,02
MnO	0,04	0,03	0,005	0,005	0,02	0,02	0,02	0,01	0,02	0,02	0,02
MgO	0,71	0,69	0,14	0,09	0,52	0,48	0,32	0,27	0,82	0,7	0,73
CaO	2,52	2,46	1,58	1,3	2,15	2,11	2,01	1,78	2,66	1,84	2,18
Na_2O	4,97	4,86	4,28	3,94	4,71	4,75	4,61	4,31	4,95	4,35	4,92
K_2O	2,79	2,82	4,47	4,62	2,83	3,17	3,23	3,82	2,36	3,64	3,09
P_2O_5	0,12	0,12	0,02	0,03	0,06	0,06	0,04	0,04	0,11	0,08	0,08
Cr_2O_3	0,001	0,001	0,001	0,001	0,001	0,001	0,001	0,001	0,001	0,003	0,002
LOI	0,2	0,2	0,3	0,3	0,3	0,3	0,5	0,6	0,3	1,1	0,4
Total	99,76	99,74	99,78	99,91	99,77	99,8	99,78	99,86	99,76	99,71	99,77
A/CNK	1,55	1,54	1,48	1,46	1,56	1,54	1,54	1,49	1,59	1,50	1,52
Cs	2,2	2,7	1,2	1,3	2,3	1,3	1,8	1	1,8	2,2	2
Rb	107,8	114	116	112,4	77,1	77,3	103,3	89,1	84,4	123,3	104,4
Ba	1206	1154	1524	541	1248	1248	1220	1014	1130	1671	1359
Th	14,9	13,9	2,4	56,5	5,7	6,9	10,6	2,6	12,5	21,8	8,2
U	4,9	2,6	1	27,5	2,4	1,5	2,5	0,6	1,2	4,2	2
Nb	2,1	2,7	0,6	0,6	2,3	0,9	2,5	1,7	2,2	2,8	3
Ta	0,2	0,2	0,05	0,05	0,05	0,05	0,3	0,05	0,2	0,05	0,1
La	37,8	37	6,2	31,2	13,7	14,5	18,2	6,7	39,9	27,9	18,8
Ce	74,3	66,4	12,3	62,8	25,3	28,5	33,5	13,3	74,3	51,7	34,2
Pr	7,2	6,91	1,12	6	2,67	2,67	3,5	1,26	7,33	5,24	3,52
Sr	728,4	702,1	582	181,1	565,5	597,7	589,3	416,2	782,5	646,5	660,7
Nd	23,1	24,3	3,6	19,2	9	9	12,2	4,2	25,8	17,6	13,2
Sm	3,29	3,1	0,56	3,33	1,41	1,48	1,72	0,77	3,12	2,52	1,86
Zr	147,3	150,9	52,2	84,6	104,6	86,2	92,2	71,5	144,6	111,8	118,2
Hf	3,7	3,8	2,2	3,5	3	2,6	3,1	2,4	3,2	3,1	3,7
Eu	0,92	0,87	0,48	0,48	0,54	0,5	0,63	0,46	0,82	0,91	0,86
Gd	1,76	1,66	0,34	2,05	0,79	0,82	0,95	0,47	1,55	1,23	1,17
Tb	0,2	0,2	0,04	0,26	0,1	0,1	0,14	0,05	0,19	0,15	0,13
Dy	0,71	0,76	0,16	1,09	0,41	0,38	0,65	0,23	0,73	0,59	0,55
Y	3	3,4	0,6	3,5	1,9	1,7	3,3	0,9	3	2,5	2,4

Ho	0,12	0,1	0,02	0,15	0,06	0,06	0,1	0,03	0,09	0,08	0,07
Er	0,27	0,26	0,07	0,33	0,17	0,17	0,28	0,11	0,23	0,16	0,19
Tm	0,04	0,04	0,01	0,05	0,03	0,03	0,05	0,02	0,03	0,03	0,03
Yb	0,18	0,19	0,05	0,24	0,16	0,12	0,29	0,06	0,19	0,19	0,17
Lu	0,03	0,03	0,01	0,05	0,03	0,02	0,05	0,01	0,03	0,03	0,03

Apêndice 02: Continuação.